Classical versus quantum errors in quantum computation of dynamical systems

Davide Rossini*
Center for Nonlinear and Complex Systems, Università degli Studi dell'Insubria and NEST-INFM & Scuola Normale Superiore, Piazza dei Cavalieri 7, 56126 Pisa, Italy

Giuliano Benenti† and Giulio Casati‡
Center for Nonlinear and Complex Systems, Università degli Studi dell'Insubria and Istituto Nazionale per la Fisica della Materia, Unità di Como, Via Valleggio 11, 22100 Como, Italy
(Received 31 May 2004; published 22 November 2004)

We analyze the stability of a quantum algorithm simulating the quantum dynamics of a system with different regimes, ranging from global chaos to integrability. We compare, in these different regimes, the behavior of the fidelity of quantum motion when the system's parameters are perturbed or when there are unitary errors in the quantum gates implementing the quantum algorithm. While the first kind of errors has a classical limit, the second one has no classical analog. It is shown that, whereas in the first case ("classical errors") the decay of fidelity is very sensitive to the dynamical regime, in the second case ("quantum errors") it is almost independent of the dynamical behavior of the simulated system. Therefore, the rich variety of behaviors found in the study of the stability of quantum motion under "classical" perturbations has no correspondence in the fidelity of quantum computation under its natural perturbations. In particular, in this latter case it is not possible to recover the semiclassical regime in which the fidelity decays with a rate given by the classical Lyapunov exponent.

DOI: 10.1103/PhysRevE.70.056216 PACS number(s): 05.45.Mt, 03.67.Lx

I. INTRODUCTION

Fidelity is a very convenient tool to characterize the stability of quantum computation. It is defined as $f(t) = |\langle \psi(t) | \psi_\epsilon(t) \rangle|^2$, where the two state vectors $|\psi(t)\rangle$ and $|\psi_\epsilon(t)\rangle$ are obtained by evolving the same initial state $|\psi_0\rangle$, under ideal or imperfect quantum gates, respectively. Here ϵ measures the imperfection strength and we assume that the perturbed gates are still unitary. If the fidelity is close to 1, the results of the quantum computation are close to the ideal ones, while, if f is significantly smaller than 1, then quantum computation does not provide reliable results.

More generally the fidelity (also called the Loschmidt echo) is a quantity of central interest in the study of the stability of dynamical systems under perturbations [1–18]. The decay of fidelity in time exhibits a rich variety of different behaviors, from Gaussian to exponential or power-law decay, depending, e.g., on the chaotic or integrable nature of the system under investigation, on the initial state (coherent state, mixture, etc.), and, for integrable systems, on the shape of the perturbation and on initial conditions. In particular, in the chaotic, semiclassical regime and for strong enough perturbations, it has been shown that the decay rate is perturbation independent and determined by the Kolmogorov-Sinai entropy, related to the Lyapunov exponent of classical chaotic dynamics [2].

On the other hand, the simulation of the quantum dynamics of models describing the evolution of complex systems promises to become the first application in which a quantum computer with only a few tens of qubits may outperform a classical computer. Indeed, efficient quantum algorithms simulating the quantum evolution of dynamical systems like the baker's map [19], the kicked rotator [20], and the sawtooth map [21] have been found, and important physical quantities could be extracted from these models already with less than 10 qubits [22–24]. Therefore, these quantum algorithms may constitute the ideal software for short- and medium-term quantum computers operating with a small number of qubits and the most suitable testing ground for investigating the limits to quantum computation due to imperfections and decoherence effects. In this context, we point out that the fidelity of quantum computation has been evaluated for the quantum baker's map using a three-qubit NMR-based quantum processor [25]. We also note that efficient quantum algorithms to compute the fidelity have been proposed in Refs. [26,27].

From the viewpoint of computational complexity, the following question naturally arises: given a generic dynamical system, is it possible to find its solution at time t efficiently, including into consideration unavoidable computational errors? We recall that the classical dynamics of chaotic systems is characterized by exponential sensitivity: any amount of error in determining the initial conditions diverges exponentially, with the rate given by the largest Lyapunov exponent λ. This means that, when following a given orbit, one digit of accuracy is lost per suitably chosen unit of time. Therefore, to be able to follow one orbit up to time t accurately, we must input $O(t)$ bits of information to determine initial conditions. On the other hand, the orbit of a non-chaotic system is much easier to simulate, since errors only grow linearly with time. Owing to the exponential instability, classical chaotic dynamics is in practice irreversible, as shown by

*Electronic address: d.rossini@sns.it
†Electronic address: giuliano.benenti@uninsubria.it
‡Electronic address: giulio.casati@uninsubria.it; URL: http://scienze-como.uninsubria.it/complexcomo

Loschmidt echo numerical simulations of Ref. [28]: if, starting from a given classical distribution in phase space, we simulate the dynamical evolution up to time t and then, by inverting at time t all the momenta, we follow the backward evolution, we do not recover the initial distribution at time $2t$. This is because any amount of numerical error in computer simulations rapidly effaces the memory of the initial conditions. On the contrary, the same numerical simulations in the quantum case show that time reversibility is preserved in the presence of small errors.

In view of the above considerations, it is natural to inquire whether the degree of stability of a quantum algorithm depends on the nature (chaotic or nonchaotic) of the simulated dynamics. We will show that the decay of the fidelity of a quantum algorithm in the presence of perturbations in the quantum gates is almost independent of the dynamical behavior of the simulated system.

In this paper, we will consider a quantum system, the so-called sawtooth map, which can be simulated efficiently on a quantum computer and whose underlying classical dynamics, depending on system's parameters, can be chaotic or nonchaotic. We will outline the main differences that occur in calculating the fidelity decay with "classical" and "quantum" perturbations on the dynamical system.

(i) By *classical perturbations*, we mean perturbations of the system's parameters that have a classical limit. For instance, in this paper we perturb, at each map step of the sawtooth model, the kicking strength k by a small amount $\delta k(t) \ll k$, where t measures the number of map iterations. Note that this kind of perturbation, when applied to the classical motion, disturbs a given orbit by a small amount at each map step and therefore, to some extent, mimics the presence of round-off errors in a classical computer.

(ii) By *quantum perturbations*, we mean errors introduced at each quantum gate (in this paper, we consider unitary, memoryless errors). These quantum errors are unavoidable during a quantum computation, due to the imperfect control of the quantum computer hardware, and they do not have a classical analog. We will show that the fidelity decay evaluated with quantum errors is not capable of distinguishing between the classically integrable or chaotic nature of the simulated dynamics, being essentially independent of it.

This paper is organized as follows. In Sec. II, we briefly describe the sawtooth map model and a quantum algorithm which efficiently simulates it. We also introduce our quantum and classical error models and discuss how to efficiently evaluate the fidelity on a quantum computer. In Sec. III, based on extensive numerical simulations, we analyze the differences between the fidelity decay in the presence of classical and quantum error. Finally, in Sec. IV we present our conclusions.

II. PERTURBED QUANTUM SAWTOOTH MAP MODEL

In order to illustrate the striking differences between the fidelity decays induced by classical and quantum errors, here we consider the quantum sawtooth map model. This map is one of the most extensively studied dynamical systems, since it exhibits a rich variety of different dynamical regimes, ranging from integrability to chaos, and interesting physical phenomena like normal and anomalous diffusion, dynamical localization, and cantori localization [29–33].

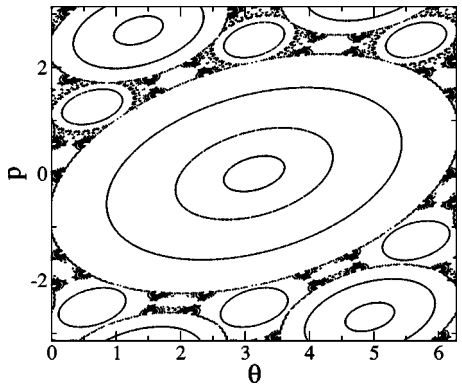

FIG. 1. Poincaré cross sections for the classical sawtooth map in the quasi-integrable regime at $K=-0.5$. We show seven trajectories inside the integrable islands and a single trajectory filling the anomalously diffusive region.

The sawtooth map is a periodically driven dynamical system, described by the Hamiltonian

$$H(\theta,n,t) = \frac{n^2}{2} - \frac{k(\theta-\pi)^2}{2} \sum_{j=-\infty}^{+\infty} \delta(t-jT), \tag{1}$$

where (n,θ) are the conjugated action-angle variables ($0 \leqslant \theta < 2\pi$). The time evolution $t \to t+T$ of this system is classically described by the map

$$\overline{n} = n + k(\theta-\pi), \quad \overline{\theta} = \theta + T\overline{n}, \tag{2}$$

where the overbars denote the variables after one map iteration. By rescaling $n \to p = Tn$, the classical dynamics is seen to depend only on the parameter $K=kT$. The classical motion is stable for $-4 \leqslant K \leqslant 0$ and completely chaotic for $K<-4$ and $K>0$: the maximum Lyapunov exponent is $\lambda = \ln[(2+K+\sqrt{K^2+4K})/2]$ for $K>0$, $\lambda = \ln|(2+K-\sqrt{K^2+4K})/2|$ for $K<-4$, and $\lambda=0$ for $-4 \leqslant K \leqslant 0$. As shown in Fig. 1, in the stable, quasi-integrable regime, the phase space has a complex structure of elliptic islands down to smaller and smaller scales. Note that the integrable islands are surrounded by a nonintegrable region and that each trajectory diffuses (anomalously) in this region. The cases $K=0,-1,-2,-3,-4$ are integrable.

The quantum evolution in one map iteration is described by the unitary operator $\hat{U}$:

$$|\overline{\psi}\rangle = \hat{U}|\psi\rangle = e^{-iT\hat{n}^2/2} e^{ik(\hat{\theta}-\pi)^2/2} |\psi\rangle, \tag{3}$$

where $[\hat{\theta},\hat{n}] = i$, $\hat{n} = -i\partial/\partial\theta$, and $|\psi(\theta+2\pi)\rangle = |\psi(\theta)\rangle$. Note that we have set $\hbar=1$. We study this map on the torus $0 \leqslant \theta < 2\pi$, $-\pi \leqslant p < \pi$. The effective Planck constant is given by $\hbar_{\text{eff}} = T$. Indeed, if we consider the operator $\hat{p} = T\hat{n}$ ($\hat{p}$ is the quantization of the classical rescaled action p), we have

$$[\hat{\theta},\hat{p}] = T[\hat{\theta},\hat{n}] = iT = i\hbar_{\text{eff}}. \tag{4}$$

The classical limit $\hbar_{\text{eff}} \to 0$ is obtained by taking $k \to \infty$ and $T \to 0$, while keeping $K = kT$ constant. We consider Hilbert spaces of dimension $N = 2^{n_q}$, where n_q is the number of qubits, and set $T = 2\pi/N$. Therefore, $\hbar_{\text{eff}} \propto 1/N = 1/2^{n_q}$ drops to zero exponentially with the number of qubits.

The operator $\hat{U}$ can be written as the product of two operators $\hat{U}_k = e^{ik(\hat{\theta}-\pi)^2/2}$ and $\hat{U}_T = e^{-iT\hat{n}^2/2}$. Since $\hat{U}_k$ is diagonal in the θ representation, while $\hat{U}_T$ is diagonal in the n representation, the most convenient way to simulate map (3) on a classical computer is based on the forward-backward fast Fourier transform between θ and n representations and requires $O(N \log N)$ operations per map iteration. The quantum computation takes advantage of the quantum Fourier transform and needs $O((\log N)^2)$ one- and two-qubit gates to accomplish the same task [21,22]. More precisely, it needs $2n_q$ Hadamard gates and $3n_q^2 - n_q$ controlled-phase shift gates. Therefore, the resources required to the quantum computer to simulate the evolution of the sawtooth map are only logarithmic in the system size N, and there is an exponential speedup, as compared to the best known classical computation.

Any experimental realization of a quantum computer has to face the problem of errors, which inevitably set limitations to the accuracy of the implemented algorithms. These errors can be due to unwanted couplings with the environment or to imperfections in the quantum hardware. In this paper, we limit ourselves to consider *unitary errors*, modeled by *noisy gates*. Such noise results from the imperfect control of the quantum computer. For instance, in a NMR quantum computer the logic gates on qubits are simulated by applying magnetic fields to the system. If the direction or the intensity of the fields is not correct, a slightly different gate is applied, though it remains unitary. In ion-trap quantum processors, laser pulses are used to implement sequences of quantum gates [34]. Fluctuations in the duration of each pulse induce unitary errors, which accumulate during a quantum computation.

As we have stated above, the implementation of the quantum algorithm for the sawtooth map requires controlled-phase shift and Hadamard gates [21,22]. We choose to perturb them as follows. Controlled-phase shift gates are diagonal in the computational basis and act nontrivially only on the four-dimensional Hilbert subspace spanned by two qubits. In this subspace, we write each controlled-phase shift gate as $\tilde{C} = \mathcal{E}C$, where C is the ideal gate and the diagonal perturbation $\mathcal{E}$ is given by $\mathcal{E} = \text{diag}(e^{i\epsilon_0}, e^{i\epsilon_1}, e^{i\epsilon_2}, e^{i\epsilon_3})$. Therefore, the unitary error operator $\mathcal{E}$ introduces unwanted phases. The Hadamard gate can be seen as a rotation of the Bloch sphere through an angle $\delta = \pi$ about the axis $\hat{u}_0 = (\sin\theta_0 \cos\phi_0, \sin\theta_0 \sin\phi_0, \cos\theta_0)$, where $\theta_0 = \pi/4$ and $\phi_0 = 0$, so that $\hat{u}_0 = (1/\sqrt{2}, 0, 1/\sqrt{2})$. Since each one-qubit gate can be seen as a rotation about some axis $\hat{u}$, unitary errors tilt the rotation angle: $\hat{u}_0 \to \hat{u} = (\sin\theta\cos\phi, \sin\theta\sin\phi, \cos\theta)$, where $\theta = \theta_0 + \nu_1$ and $\phi = \phi_0 + \nu_2$. We assume that the dephasing parameters ϵ_i, ν_j $(i = 1, \ldots, 4,\ j = 1, 2)$, are randomly and uniformly distributed in the interval $[-\epsilon, \epsilon]$. We also assume

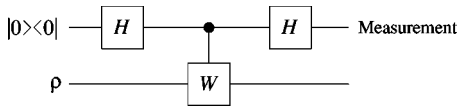

FIG. 2. Scattering circuit. The top line denotes a single ancillary qubit, the bottom line a set of n_q qubits, H the Hadamard gate, and W a unitary transformation.

that the errors affecting different quantum gates are completely *uncorrelated*: every time we apply a noisy gate, the dephasing parameters randomly fluctuate in the (fixed) interval $[-\epsilon, +\epsilon]$. We note that the memoryless unitary error model has been widely investigated in the literature; see, e.g., Refs. [35–39].

We will compare the effect of noisy gates ("quantum errors") with that of *randomly fluctuating perturbations* in the system's parameters ("classical errors"). Here we choose to perturb the kicking strength k in Eq. (2) as follows: at each map step, k is slightly changed by a small amount $\delta k(t)$, which is randomly chosen in the interval $[-\delta k, \delta k]$. Consequently, $\delta K(t) \equiv T\delta k(t) \in [-\delta K, +\delta K]$, where $\delta K \equiv T\delta k$. As we have discussed in the Introduction, this perturbation models, to some extent, the effect of round-off errors in classical computation.

We will consider the following initial conditions.

(i) A *coherent Gaussian wave packet*

$$|\psi_0\rangle_G = A \sum_{n=0}^{N-1} e^{-(n-n_0)^2/2\sigma^2 + i(n-n_0/2)\theta_0} |n\rangle, \tag{5}$$

where (θ_0, n_0) is the center of the wave packet $(\langle\hat{\theta}\rangle = \theta_0, \langle\hat{n}\rangle = n_0)$, A a normalization constant, and $\sigma^2 = (\Delta n)^2 \equiv \langle(\hat{n} - \langle\hat{n}\rangle)^2\rangle$ the variance in the momentum representation [40]. We choose $\sigma^2 = N/(2\pi L)$ in order to obtain an equal value for the variances in p and in θ—namely, $\Delta\theta\Delta p = \hbar_{\text{eff}}$, with $\Delta\theta = \Delta p = \sqrt{\hbar_{\text{eff}}}$. The wave vector (5) is the closest quantum analog of a classical probability density, localized in a small region of the phase space, centered in (θ_0, p_0) and of width σ. We point out that, as shown in Ref. [41], it is possible to prepare efficiently a coherent state on a quantum computer.

(ii) A *random wave vector* $|\psi_0\rangle_R = \Sigma_{n=1}^{N} c_n |n\rangle$, where the coefficients c_n have amplitudes of the order of $1/\sqrt{N}$ (to assure the normalization of the wave vector) and random phases. This state has no classical analog.

The fidelity of quantum motion can be efficiently evaluated on a quantum computer, as discussed in Ref. [26]. Here we show an alternative method, based on the scattering circuit drawn in Fig. 2 [42,43]. This circuit has various important applications in quantum computation, including quantum-state tomography and quantum spectroscopy [43]. It ends up with a polarization measurement of just the ancillary qubit. We measure σ_z or σ_y and the average values of these observables are

$$\langle\sigma_z\rangle = \text{Re}[\text{Tr}(\hat{W}\rho)], \quad \langle\sigma_y\rangle = \text{Im}[\text{Tr}(\hat{W}\rho)], \tag{6}$$

where $\langle\sigma_z\rangle$ and $\langle\sigma_y\rangle$ are the expectation values of the Pauli spin operators $\hat{\sigma}_z$ and $\hat{\sigma}_y$ for the ancillary qubit, and $\hat{W}$ is a

unitary operator acting on n_q qubits, initially prepared in the state ρ (see Fig. 2). These two expectation values can be obtained (up to statistical errors) if one runs several times the scattering circuit. If we set $\rho=|\psi_0\rangle\langle\psi_0|$ and $\hat{W}=(\hat{U}^t)^\dagger\hat{U}_\epsilon^t$, it is easy to see that

$$f(t)=|\langle\psi_0|(\hat{U}^t)^\dagger\hat{U}_\varepsilon^t|\psi_0\rangle|^2=|\mathrm{Tr}(\hat{W}\rho)|^2=\langle\sigma_z\rangle^2+\langle\sigma_y\rangle^2. \quad (7)$$

For this reason, provided that the quantum algorithm implementing $\hat{U}$ is efficient, as is the case for the quantum sawtooth map, the fidelity can be efficiently computed by means of the circuit shown in Fig. 2.

III. RESULTS AND DISCUSSION

Hereafter we will call $f_c(t)$ and $f_q(t)$ the fidelity decays induced by classical or quantum errors, respectively.

Let us first consider the fidelity decay $f_c(t)$, obtained under fluctuating perturbations in the parameter k of the sawtooth map. We will show that, under this type of perturbation, the fidelity decay exhibits a marked dependence on the simulated dynamics. In particular, qualitatively different behaviors are observed depending on the chaotic or nonchaotic motion.

We first consider the *quasi-integrable regime* $-4\leqslant K\leqslant 0$. In this case the sawtooth map behaves, inside the main integrable island with fixed point $(\theta,p)=(\pi,0)$ (see Fig. 1), as a harmonic oscillator, with characteristic frequency $\nu_K=\omega_K/2\pi=\sqrt{-K}/2\pi$. Therefore, in the semiclassical regime the quantum motion of coherent wave packets residing inside integrable islands closely follows the harmonic evolution of the corresponding classical trajectories. In the central island this motion has period $T=2\pi/\sqrt{-K}$, while in the outer islands the period is multiplied by a factor which depends on the order of the corresponding resonances (for example, the two upper islands in Fig. 1 correspond to a second-order resonance, and inside them the period is doubled).

Since the chosen perturbation affects the parameter K, the fidelity $f_c(t)$ is obtained as the overlap of two wave packets which move inside an integrable island with slightly different frequencies. In this case, we know [9,44] that for a static perturbation $[\delta K(t)=\delta K]$ the centers of the two wave packets separate ballistically (linearly in time) and a very fast decay of quantum fidelity is expected as far as the distance between the centers of the two packets becomes larger than their width σ. The type of decay is related to the shape of the initial wave packet. In particular, for a Gaussian wave packet a Gaussian decay is expected. If $\delta\nu_K\equiv\nu_{K+\delta K}-\nu_K$ denotes the frequency separation between perturbed and unperturbed motion, the Gaussian decay takes place after a time $t_s\propto\sigma/\delta\nu_K$.

In this paper, we consider the case of a randomly fluctuating perturbation $\delta K(t)\in[-\delta K,\delta K]$. Therefore, the frequency $\nu_{K+\delta K(t)}$ of a classical trajectory following the perturbed dynamics is not constant. The relative displacement of this orbit with respect to the one described by the unperturbed dynamics (with a frequency ν_K) is approximately given by a Brownian motion. The separation between the two orbits is proportional to the frequency difference $\delta\nu_K$. In this case the fidelity decay is again Gaussian, but in general it shows large random fluctuations from the Gaussian profile (see, for example, the upper curve in Fig. 3), which depend on the noise realization. Moreover, the distance between the centers of the two wave packets grows $\propto\sqrt{\delta\nu_K t}$, and therefore the Gaussian decay starts after a time scale $t_s\propto\sigma^2/\delta\nu_K$.

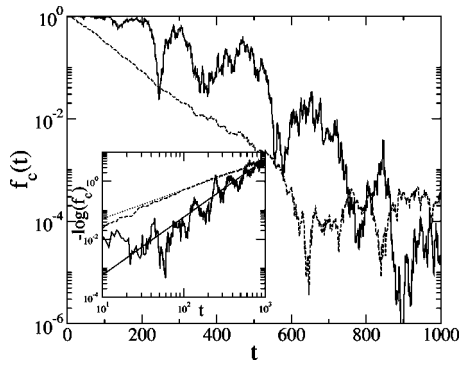

FIG. 3. Fidelity decay for the quantum sawtooth map with $n_q=12$ qubits, in the presence of a classical fluctuating perturbation in the k parameter. The initial condition is a Gaussian wave packet centered in $(\theta_0,p_0)=(1,0)$. The upper curve shows the behavior in the quasi-integrable regime $K=-0.5$, with maximum perturbation strength $\delta K=4\times10^{-3}$; the lower one is obtained by simulating the map in the chaotic regime $K=0.5$, with $\delta K=2\times10^{-4}$. In the inset we plot the same curves in a graph showing $-\log(f_c)$ versus time. The straight lines correspond to exponential fidelity decay ($-\log f_c\propto t$, upper line) and Gaussian decay ($-\log f_c\propto t^2$, lower line). Here and in the following figures the logarithms are decimal.

Moreover, the fidelity decay depends not only on the shape of the initial state, but also on its position. Indeed, inside any integrable island the frequency's perturbation $\delta\nu_K=\nu_{K+\delta K}-\nu_K\approx\delta K/4\pi\sqrt{-K}$ is independent of the position of the wave packet in phase space. Since larger orbits imply a larger velocity and, consequently, a larger relative ballistic motion of the two wave packets, the fidelity drops faster when we move far from the center of the integrable islands. This is confirmed by our numerical data (not shown here).

In the *chaotic regime*, the fidelity $f_c(t)$ always decays exponentially, and an example of such decay is given in Fig. 3. For small perturbations, in the chaotic regime the decay rate $\Gamma\propto(\delta K)^2$, as predicted by the Fermi golden rule. However, if the perturbation is strong enough, the fidelity decay follows a semiclassical regime, in which the decay rate is perturbation independent and equal to the Lyapunov exponent of the underlying classical dynamics (see inset of Fig. 4). The condition to observe the Lyapunov decay is that the perturbation be quantally strong—namely, that it couple many levels $(\delta k>1)$—but classically weak $(\delta k\ll k)$.

To summarize, the fidelity decay induced by classical perturbations strongly depends on the dynamical regime, chaotic or integrable. The two qualitatively different behaviors (exponential or Gaussian decay) are shown in Fig. 3. Notice also that the regular dynamics turns out to be much more stable than the chaotic one (to represent both cases in the same figure, the perturbation value chosen in the chaotic case is 20 times smaller than the one chosen in the integrable case).

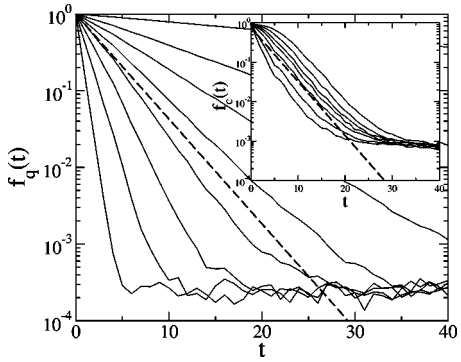

FIG. 4. Fidelity decay for noisy gates in the sawtooth map with $K=0.1$, $n_q=12$. From right to left $\epsilon=1.5\times10^{-2}$, 3×10^{-2}, 4×10^{-2}, 5×10^{-2}, 6×10^{-2}, 7.5×10^{-2}, 10^{-1}, 1.5×10^{-1}. Inset: fidelity decay for uncorrelated perturbations in the parameter k. From right to left, $\delta K=T\delta k=3\times10^{-3}$, 5×10^{-3}, 7.5×10^{-3}, 10^{-2}, 1.5×10^{-2}, 3×10^{-2}, 5×10^{-2}. In both graphs, data are averaged over 50 initial Gaussian wave packets. The two dashed lines show the Lyapunov exponential decay: $f(t)=e^{-\lambda t}$, where $\lambda\approx0.315$ is the classical Lyapunov exponent corresponding to $K=0.1$.

We now analyze the fidelity behavior in the presence of natural errors for quantum computation—namely, *random unitary perturbations* of amplitude ϵ on *quantum gates*—following the noise model described in Sec. II.

As shown in Figs. 4 and 5, in the *chaotic regime* the fidelity $f_q(t)$ drops exponentially, with a rate $\Gamma\propto\epsilon^2 n_q^2$ [45]. This decay can be understood from the Fermi golden rule: each noisy gate transfers a probability of order ϵ^2 from the ideal unperturbed state to other states. Due to the fact that perturbations acting on two different gates are completely uncorrelated, an exponential decay rate proportional to ϵ^2 and to the number of gates $n_g=3n_q^2+n_q$ required to implement one step of the sawtooth map is expected:

$$f_q(t)\simeq e^{-\Gamma t}\simeq e^{-C\epsilon^2 n_g t}, \tag{8}$$

where $C\approx0.28$ is a constant which we have computed from our numerical data. We have determined the characteristic time scale t_f for fidelity decay from the condition $f_q(t_f)=A=0.9$ (note that the value chosen for A is not crucial). Our numerical calculations, shown in Fig. 5, clearly demonstrate that

$$t_f\propto\frac{1}{\epsilon^2 n_q^2}, \tag{9}$$

in agreement with Eq. (8).

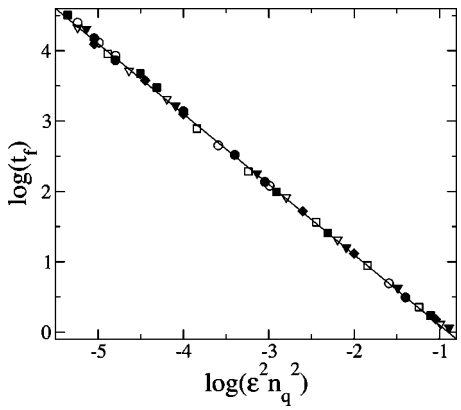

FIG. 5. Characteristic time scale t_f for the fidelity decay, determined by the condition $f(t_f)=0.9$, in the sawtooth map at $K=5$, for the case of random noise errors in quantum gates. The data are obtained for different perturbation strengths ϵ and number of qubits: $n_q=4$ (open circles), 5 (solid circles), 6 (open squares), 7 (solid squares), 8 (open triangles), 9 (solid triangles), and 10 (solid diamonds). The straight line shows the dependence $t_f\simeq0.126/\epsilon^2 n_q^2$, corresponding to the exponential fidelity decay (8), with $C\approx0.28$. The initial state is in all cases a Gaussian wave packet and data are averaged over 50 noise realization.

The fidelity decay in the chaotic regime *always* follows the exponential behavior predicted by the Fermi golden rule. Therefore, in contrast with the case of classical errors, there is no saturation of the decay rate to the largest Lyapunov exponent of the system (see Fig. 4).

This result can be understood from the *nonlocality* of quantum errors: each noisy gate can make direct transfer of probability on a large distance in phase space. This is a consequence of the binary encoding of the discretized angle and momentum variables. For instance, we represent the momentum eigenstates $|n\rangle$ $(-N/2\leqslant n<N/2)$ in the computational basis as $|\alpha_{n_q}\cdots\alpha_2\alpha_1\rangle$, where $\alpha_j\in\{0,1\}$ and $n=-N/2+N\sum_{j=1}^{n_q}\alpha_j 2^{-j}$. If we take, say, $n_q=6$ qubits ($N=2^6=64$), the state $|000000\rangle$ corresponds to $|n=-32\rangle$ $(p=-\pi)$, $|000001\rangle$ to $|n=-31\rangle$ $[p=-\pi+2\pi(1/2^6)]$, and so on until $|111111\rangle$, corresponding to $|n=31\rangle$ $[p=-\pi+2\pi(63/2^6)]$. Let us consider the simplest quantum error, the bit flip: if we flip the less significant qubit $(\alpha_1=0\leftrightarrow1)$, we exchange $|n\rangle$ with $|n+1\rangle$ (mod N), while, if we flip the most significant qubit $(\alpha_{n_q}=0\leftrightarrow1)$, we exchange $|n\rangle$ with $|n+32\rangle$ (mod N). It is clear that this latter error transfers probability very far in phase space and cannot be reproduced by classical local errors. Therefore, no semiclassical regime for the fidelity decay is expected with quantum errors. In particular, the nonlocality of perturbations makes the fidelity insensitive to the rate of local exponential instability, given by the Lyapunov exponent.

The most striking feature of the fidelity decay induced by quantum errors is that it is substantially independent of the chaotic or nonchaotic nature of the underlying classical dynamics. An example of this behavior is shown in Fig. 6 and strongly contrasts with what obtained by perturbing the system's parameters (see Fig. 3). In particular, the fidelity decay for integrable dynamics is exponential, as shown in Fig. 6. We note that in Ref. [26] it was pointed out that even classically regular models can exhibit an exponential fidelity decay. If we start from a Gaussian wave packet, integrable dynamics turns out to be a little more stable than chaotic dynamics: we numerically obtained a ratio of the decay rates in the chaotic and in the integrable case which oscillates between 1.15 and 1.4, for different values of n_q between 5 and 16 and for various ϵ ranging from 10^{-5} to 10^{-1}.

We stress that the smaller decay rate obtained when we evolve a Gaussian wave packet inside an integrable island is not due to the lack of exponential instability but simply to

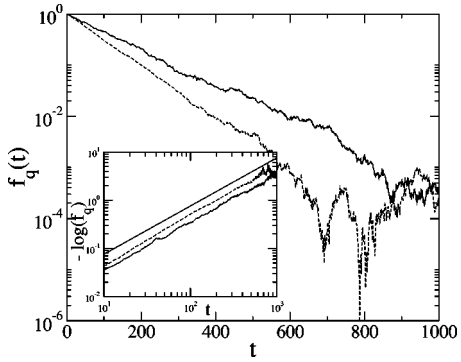

FIG. 6. Fidelity decay for the quantum sawtooth map simulated with $n_q=12$ qubits, in the presence of uncorrelated unitary quantum errors with maximum perturbation strength $\epsilon=10^{-2}$. As initial condition we consider a Gaussian wave packet peaked in $(\theta_0,p_0)=(1,0)$. The upper curve shows the behavior in the quasi-integrable regime $K=-0.5$, while the lower one is obtained by simulating the map in the chaotic region $K=0.5$. In the inset we plot the same curves, showing $-\log(f_q)$ versus time. The solid line corresponds to exponential fidelity decay, that is $-\log f_q \propto t$.

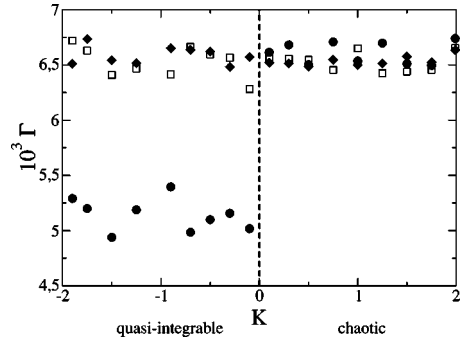

FIG. 7. Dependence of the fidelity decay rate, induced by quantum uncorrelated unitary perturbations, on K, for $n_q=9$, $\epsilon=10^{-2}$. The dashed line separates the quasi-integrable region $-4\leqslant K\leqslant 0$ from the chaotic region $K>0$. As initial condition we choose (i) a Gaussian wave packet centered in $(\theta_0,p_0)=(1,0)$ (circles) (note that for $-4<K<0$ this packet is inside the main integrable island), (ii) a Gaussian packet centered in $(\theta_0,p_0)=(0,0)$ (squares)—that is, residing in the diffusive region, and (iii) a random wave function (diamonds). All data are obtained after averaging over 25 different noise realizations.

the fact that the dynamics preserves the coherence of the wave packet. This can be clearly seen from the data of Fig. 7.

(i) In the *chaotic regime* $K>0$ (Lyapunov exponent $\lambda>0$), the fidelity decay rate is independent of the initial state (Gaussian packet or random state) and of the rate of exponential instability. Indeed, the decay rate is independent of K, while λ depends on K.

(ii) In the *quasi-integrable regime* $-4<K<0$ (Lyapunov exponent $\lambda=0$), only in the case in which we choose as initial state a Gaussian packet placed inside an integrable island do we obtain a fidelity decay rate smaller than in the chaotic case. On the other hand, if we start from a random state or if we place the Gaussian wave packet inside the anomalously diffusive region, we obtain the same decay rate as in the chaotic case.

From these results, we conclude that the decay rate does not depend on the value of the Lyapunov exponent. In short, the decay of the fidelity due to noisy gates is *independent of the presence or lack of exponential instability* [46]. We point out that we have checked that this statement remains valid also for static errors, like in the case in which the dephasing parameters ϵ_i, ν_j appearing in our noise model are time independent.

IV. CONCLUSIONS

In this paper, we have compared the effects of classical and quantum errors on the stability of quantum motion. The main result is that, while the fidelity decay under classical errors strongly depends on the dynamical nature of the system under investigation and on initial conditions, quantum errors act in a way essentially independent of the system's dynamics. This practical insensitivity to the dynamics is eventually a consequence of the intrinsic nonlocality of the errors that naturally affect the quantum computation. As a consequence, the rich variety of behaviors found in the study of the stability of quantum motion under perturbations of the system's Hamiltonian [1–18] has no correspondence in the fidelity of quantum computation under its natural perturbations. The stability of quantum computation is essentially independent of the chaotic or integrable behavior of the simulated dynamics. This conclusion is simply based on the nonlocality of quantum errors and therefore we expect that it remains valid also in the case of nonunitary quantum noise and/or when errors, correlated or memoryless, act not only on the qubits on which we apply a quantum gate but on all the qubits that constitute the quantum computer.

ACKNOWLEDGMENTS

We gratefully acknowledge useful discussions with Dima Shepelyansky. This work was supported in part by EC Contract Nos. IST-FET EDIQIP and RTN QTRANS, the NSA and ARDA under ARO Contract No. DAAD19-02-1-0086, the PRIN 2002 "Fault tolerance, control and stability in quantum information precessing," and the PA INFM "Weak chaos: Theory and applications."

[1] A. Peres, Phys. Rev. A **30**, 1610 (1984).
[2] R.A. Jalabert and H.M. Pastawski, Phys. Rev. Lett. **86**, 2490 (2001).
[3] F.M. Cucchietti, H.M. Pastawski, and D.A. Wisniacki, Phys. Rev. E **65**, 045206(R) (2002).
[4] Ph. Jacquod, P.G. Silvestrov, and C.W.J. Beenakker, Phys. Rev. E **64**, 055203(R) (2001).
[5] N.R. Cerruti and S. Tomsovic, Phys. Rev. Lett. **88**, 054103 (2002).
[6] V.V. Flambaum and F.M. Izrailev, Phys. Rev. E **64**, 036220 (2001).
[7] G. Benenti and G. Casati, Phys. Rev. E **65**, 066205 (2002).
[8] D.A. Wisniacki and D. Cohen, Phys. Rev. E **66**, 046209 (2002).
[9] T. Prosen, Phys. Rev. E **65**, 036208 (2002); T. Prosen and M. Žnidarič, J. Phys. A **34**, L681 (2001); **35**, 1455 (2002).
[10] Y.S. Weinstein, S. Lloyd, and C. Tsallis, Phys. Rev. Lett. **89**, 214101 (2002).
[11] W. Wang and B. Li, Phys. Rev. E **66**, 056208 (2002).
[12] Y. Adamov, I.V. Gornyi, and A.D. Mirlin, Phys. Rev. E **67**, 056217 (2003).
[13] I. Garcia-Mata, M. Saraceno, and M.E. Spina, Phys. Rev. Lett. **91**, 064101 (2003).
[14] J. Vaníček and E.J. Heller, Phys. Rev. E **68**, 056208 (2003).
[15] F.M. Cucchietti, D.A.R. Dalvit, J.P. Paz, and W.H. Zurek, Phys. Rev. Lett. **91**, 210403 (2003).
[16] M. Hiller, T. Kottos, D. Cohen, and T. Geisel, Phys. Rev. Lett. **92**, 010402 (2004).
[17] G. Veble and T. Prosen, Phys. Rev. Lett. **92**, 034101 (2004).
[18] W. Wang, G. Casati, and B. Li, Phys. Rev. E **69**, 025201 (2004).
[19] R. Schack, Phys. Rev. A **57**, 1634 (1998).
[20] B. Georgeot and D.L. Shepelyansky, Phys. Rev. Lett. **86**, 2890 (2001).
[21] G. Benenti, G. Casati, S. Montangero, and D.L. Shepelyansky, Phys. Rev. Lett. **87**, 227901 (2001).
[22] G. Benenti, G. Casati, S. Montangero, and D.L. Shepelyansky, Phys. Rev. A **67**, 052312 (2003).
[23] A.A. Pomeransky and D.L. Shepelyansky, Phys. Rev. A **69**, 014302 (2004).
[24] G. Benenti, G. Casati, and G. Strini, *Principles of Quantum Computation and Information* (World Scientific, Singapore, 2004), Vol. 1.
[25] Y.S. Weinstein, S. Lloyd, J. Emerson, and D.G. Cory, Phys. Rev. Lett. **89**, 157902 (2002).
[26] J. Emerson, Y.S. Weinstein, S. Lloyd, and D. Cory, Phys. Rev. Lett. **89**, 284102 (2002).
[27] D. Poulin, R. Blume-Kohout, R. Laflamme, and H. Ollivier, Phys. Rev. Lett. **92**, 177906 (2004).
[28] G. Casati, B.V. Chirikov, I. Guarneri, and D.L. Shepelyansky, Phys. Rev. Lett. **56**, 2437 (1986).
[29] I. Dana, N.W. Murray, and I.C. Percival, Phys. Rev. Lett. **62**, 233 (1989).
[30] F. Borgonovi, G. Casati, and B. Li, Phys. Rev. Lett. **77**, 4744 (1996).
[31] F. Borgonovi, Phys. Rev. Lett. **80**, 4653 (1998).
[32] G. Casati and T. Prosen, Phys. Rev. E **59**, R2516 (1999).
[33] A. Lakshminarayan and N. L. Balazs, Chaos, Solitons Fractals **5**, 1169 (1995).
[34] F. Schmidt-Kaler, H. Häffner, M. Riebe, S. Gulde, G.P.T. Lancaster, T. Deuschle, C. Becher, C.F. Roos, J. Eschner, and R. Blatt, Nature (London) **422**, 408 (2003).
[35] J.I. Cirac and P. Zoller, Phys. Rev. Lett. **74**, 4091 (1995).
[36] C. Miquel, J.P. Paz, and W.H. Zurek, Phys. Rev. Lett. **78**, 3971 (1997).
[37] P.H. Song and D.L. Shepelyansky, Phys. Rev. Lett. **86**, 2162 (2001).
[38] D. Shapira, S. Mozes, and O. Biham, Phys. Rev. A **67**, 042301 (2003).
[39] S. Bettelli, Phys. Rev. A **69**, 042310 (2004).
[40] Strictly speaking, the coherent state (5) should be modified in order to take into account the periodic boundary conditions along θ and n, as explained in S.-J. Chang and K.-J. Shi, Phys. Rev. A **34**, 7 (1986). However, this modification does not significantly affect the results discussed in this paper.
[41] J.P. Paz, A.J. Roncaglia, and M. Saraceno, Phys. Rev. A **69**, 032312 (2004).
[42] S.A. Gardiner, J.I. Cirac, and P. Zoller, Phys. Rev. Lett. **79**, 4790 (1997).
[43] C. Miquel, J.P. Paz, M. Saraceno, E. Knill, R. Laflamme, and C. Negrevergne, Nature (London) **418**, 59 (2002).
[44] G. Benenti, G. Casati, and G. Veble, Phys. Rev. E **68**, 036212 (2003).
[45] The exponential decay stops when the fidelity approaches $f_q(\infty)=1/N$. This saturation value is given by the inverse of the size of the Hilbert space and reflects the finiteness of the system.
[46] We obtained a further confirmation of this statement by implementing the quantum algorithm without dynamical evolution—i.e., by putting $T=0$ and $k=0$ in Eq. (3). In such a situation, we found that the fidelity drops again exponentially and the ratio between the decay rates starting from a random or a Gaussian state is the same as in the quasi-integrable regime.